Original Research

Parallel Acquisition Techniques for Accelerated Volumetric Interpolated Breath-Hold Examination Magnetic Resonance Imaging of the Upper Abdomen: Assessment of Image Quality and Lesion Conspicuity

Florian M. Vogt, MD,* Gerald Antoch, MD, Peter Hunold, MD, Stefan Maderwald, MSc, Mark E. Ladd, PhD, Jörg F. Debatin, MD, MBA, and Stefan G. Ruehm, MD

Purpose: To evaluate the impact of parallel acquisition techniques (PATs) on image quality and detection of liver metastases using three-dimensional volumetric interpolated breath-hold examination (VIBE) for clinical liver imaging.

Materials and Methods: Forty-nine patients with various primary malignancies underwent abdominal dynamic contrast-enhanced three-dimensional VIBE magnetic resonance imaging (MRI) (1.5 T) using a standard phased array coil. Recently introduced Generalized Autocalibrating Partially Parallel Acquisition (GRAPPA) and SENSitivity Encoding (mSENSE) PAT reconstruction algorithms were added to reduce scan time twofold. Overall image quality, motion, and aliasing artifacts were classified on a 5-point scale. Signal-to-noise ratio (SNR) and contrast-to-noise ratio (CNR) measurements were performed for quantitative comparison. All sequences were evaluated concerning the number of detected lesions.

Results: PAT resulted in a reduction of data acquisition time from 23 to 13 seconds. Both GRAPPA and mSENSE data sets yielded 30% less SNR (34.8 ± 14.1 and 33.1 ± 13.3, $P < 0.001$) and 35% less CNR (21.2 ± 15.0 and 20.9 ± 12.7, $P < 0.05$) in comparison to unaccelerated VIBE (SNR = 50.8 ± 20.3/CNR = 32.5 ± 19.1). Similarly, PAT revealed lower-image-quality scores than unaccelerated VIBE. GRAPPA resulted in more fold-over artifacts than mSENSE. mSENSE revealed slightly fewer motion artifacts than no PAT. The unaccelerated late-venous-phase VIBE sequence revealed 146 lesions in the same patients. Accelerated images with mSENSE reconstruction detected 138 lesions. GRAPPA revealed 127 lesions, and thus performed inferior to mSENSE.

Conclusion: At least for arrays with small numbers of elements, such as arrays used in this study, the PAT-induced reduction in scanning times must be weighed against compromises in image quality, which translate into poorer diagnostic performance regarding detection of small hepatic lesions. Thus, the PAT implementations tested in this study should probably be reserved for patients unable to hold their breaths for regular three-dimensional VIBE data sets.

Key Words: abdominal MRI; VIBE sequence; parallel acquisition techniques; image quality; lesion detection
J. Magn. Reson. Imaging 2005;21:376–382.

TO ASSURE OPTIMAL DETECTION and characterization of focal hepatic lesions, dynamic multiphase contrast-enhanced imaging has become an integral part of virtually all cross-sectional protocols covering the upper abdomen (1–3). Data acquisition needs to be sufficiently fast to ensure coverage of the entire liver within the confines of a single breath hold. Currently, fast two-dimensional gradient echo (GRE) sequences are most commonly employed (4). The need to collect the data in less than 25 seconds results in relatively thick slices of 8–10 mm, translating into partial-volume artifacts, which may obscure small hepatic lesions (5).

Recently, three-dimensional GRE imaging with uniform fat saturation has been introduced for multiphase imaging of the upper abdomen. The volumetric interpolated breath-hold examination (VIBE) technique offers minimization of partial-volume effects by providing nearly isotropic resolution. Thus, smaller hepatic lesions can be detected and characterized (6). Depending on scanner performance, three-dimensional coverage of the liver can result in breath-hold times exceeding 20–25 seconds, thereby limiting the technique's utility in patients with compromised respiratory function. This limitation may be overcome with the introduction of parallel acquisition techniques (PATs), which hold

Department of Diagnostic and Interventional Radiology, University Hospital Essen, Essen, Germany.
*Address reprint requests to: F.M.V., Department of Diagnostic and Interventional Radiology, University Hospital Essen, Hufelandstrasse 55, 45122 Essen, Germany. E-mail: florian.vogt@uni-essen.de
Received May 4, 2004; Accepted December 17, 2004.
DOI 10.1002/jmri.20288
Published online in Wiley InterScience (www.interscience.wiley.com).

the potential to reduce image acquisition times while preserving original image resolution and contrast (7–9). These techniques use spatial information contained in the component coils of a surface coil array complementary to Fourier preparation to partially replace gradient-based spatial encoding. Disadvantages of PAT relate to an associated reduction of signal-to-noise ratio (SNR), as well as the appearance of calibration errors and reconstruction artifacts, reflecting errors in the determination of the complex sensitivities inherent to the component coils.

Modern PAT algorithms, including SiMultaneous Acquisition of Spatial Harmonics (SMASH), Generalized Autocalibrating Partially Parallel Acquisition (GRAPPA), and SENSitivity Encoding (SENSE), have been shown to overcome some of these disadvantages (8,9).

The purpose of this study was to evaluate the effect of two different PAT reconstruction algorithms on three-dimensional VIBE imaging of the upper abdomen.

MATERIALS AND METHODS

Patients

Forty-nine consecutive adult patients (32 males, 17 females; mean age = 58 ± 15) with various primary malignancies were studied. Primary tumors included breast cancer (N = 9), lung cancer (N = 7), thyroid cancer (N = 7), melanoma (N = 6), pharyngeal cancer (N = 6), carcinoma of unknown primary (N = 5), malignant melanoma (N = 4), prostate cancer (N = 2), osteosarcoma (N = 2), and gastric cancer (N = 1). All patients were suspected of harboring one or more hepatic metastases and had been referred for magnetic resonance imaging (MRI) of the abdomen as part of staging protocols. MRI was performed on a 1.5-T scanner (Magnetom Sonata, Siemens Medical Systems, Erlangen, Germany) equipped with high-amplitude gradients (40 mT/m maximum amplitude) and a corresponding high slew rate (200 mT/m/msec) and a low rise time (200 μsec). All examinations, including the accelerated imaging, were conducted using a standard body phased array surface coil and spine array, each with two coil elements oriented along the head-to-feet direction for signal reception. Patients were positioned supine.

MRI

The study was performed in accordance with guidelines issued by the local institutional review board. Written informed consent was obtained from all patients, who underwent an identical imaging protocol encompassing the following sequences:

- Two-dimensional T1-weighted (TR/TE = 124/1.8 msec, flip angle = 70°, matrix/slice = 166 × 256/7 mm, acquisition time = 20 seconds)
- Fat-suppressed half-Fourier single-shot turbo spin echo (HASTE) (TR/TE = 1200/60 msec, flip angle = 140°, matrix/slice = 166 × 256/7mm, collected over 44 seconds in two breath holds)
- Dynamic, three-phase, contrast-enhanced three-dimensional VIBE (TR/TE = 3.1/1.2 msec, flip angle = 12°, axial plane, matrix/slice = 154 × 256/3 mm, slices per slab = 104, phase encoding direction = anterior-posterior).

A 250 × 400 mm field of view rendered a pixel size of 2.1 × 1.6 mm^2. Dynamic image sets were collected over 23 seconds before, as well as 20, 50, and 80 seconds following, the bolus administration of paramagnetic contrast at a dose of 0.2 mmol/kg (MultiHance, Bracco, Milan, Italy). The agent was administered with an automated injector (Medrad Spectris, Pittsburgh, PA, USA) at a rate of 2.0 mL/second and flushed with 20 mL of saline at a rate of 2.0 mL/second.

Immediately after all three unaccelerated dynamic three-dimensional VIBE imaging phases were completed (10-second delay, 113 seconds after bolus administration), an identical axial image set of the entire liver was scanned with parallel imaging. Only one raw data set was collected, but two image data sets using two different PAT reconstruction algorithms, GRAPPA and mSENSE (Siemens, Medical Solutions, Erlangen, Germany), were reconstructed from this one accelerated raw data set.

Both algorithms (GRAPPA and mSENSE) use autocalibration for coil sensitivity determination applied using 12 additional reference lines in the center of k-space (effective reference lines = 24). GRAPPA, a k-space-based reconstruction algorithm, as well as mSENSE, an imaged-based reconstruction algorithm, use the additional reference k-lines for self-calibration of coil sensitivities for each single image, thereby avoiding the need for an external reference. Hence, the potential for artifacts due to patient motion between calibration and accelerated scanning is eliminated. Twofold accelerated volumes of the liver were collected to reduce the acquisition time while keeping spatial and temporal resolution, as well as all other sequence parameters, constant.

Data Analysis

Comparative analysis was focused on the two accelerated VIBE image data sets (GRAPPA and mSENSE) and the venous (80-second) phase of the dynamic unaccelerated VIBE acquisition. Two experienced radiologists, blinded to the employed technique, analyzed in consensus the three different data sets, which were presented in random order in three viewing sessions. The three-dimensional image sets were interpreted using the multiplanar reformation (MPR) mode on a viewing station. To avoid recognition bias, the viewing sessions were separated by four weeks each. Subsequently, a consensus reading based on all imaging data (including the precontrast T1- and T2-weighted sequences, as well as the arterial and portal venous phase VIBE image sets) was completed and used as the standard of reference.

The observers evaluated the different image sets regarding number and size of focal hepatic lesions. Since only venous phase images were available, lesion characterization was not attempted. Overall image quality was rated from 1–5: 1 = uninterpretable, nondiagnostic; 2 = poor, nondiagnostic; 3 = acceptable, diagnostic; 4 = good, diagnostic; 5 = very good, diagnostic. The severity of aliasing and respiratory motion artifacts was

also rated: 1 = profound, 2 = severe, 3 = moderate, 4 = mild, 5 = imperceptible. The mean scores were compared. Data are given as mean ± SD.

For each lesion identified in each of the three data sets, signal intensity (SI) measurements were performed in three regions of interest (ROIs):

1. Within the lesion, defined as a region with the highest but also homogeneous SI (SI ROI_{lesion}).
2. Within normal liver surrounding the lesion (SI ROI_{normal}). To minimize coil inhomogenity errors, signal measurements were obtained close to the lesion.
3. In the background outside the body (air). The SD of this background SI was taken as the noise (STD_{noise}). The mean SD was calculated within four different ROIs of artifact-free areas (diameter > 15 cm).

Based on these measurements, SNR and contrast-to-noise ratio (CNR) were calculated as follows:

$$\text{SNR: } (\text{SI } ROI_{normal})/STD_{noise}$$

$$\text{CNR: } (\text{SI } ROI_{lesion} - \text{SI } ROI_{normal})/STD_{noise}$$

Since it was expected that there would be lesions with negative and positive enhancement, absolute enhancement was considered in the calculations.

The SPPS (Version 10.0 for Windows, SPSS, Inc., Chicago, IL, USA) statistics package was used for statistical analysis. For correlation concerning overall image quality, aliasing, and respiratory motion artifacts, a Wilcoxon signed rank test was performed. Comparison between measured SNR and CNR was accomplished using the paired samples *t*-test. A *P* value of <0.05 was considered to indicate statistical significance.

RESULTS

The use of both PAT techniques reduced the mean breath-hold time from 23 to 13 seconds (44% reduction in acquisition time).

Overall Image Quality

Unaccelerated VIBE image sets received significantly higher image quality ratings (mean score = 3.40 ± 1.0) than mSENSE (2.98 ± 1.0, $P = 0.0015$) and GRAPPA (2.60 ± 0.9, $P = 0.001$) (Fig. 1). GRAPPA image quality was poorer than mSENSE image quality ($P = 0.001$). Of 49 unaccelerated image sets, 8 (16%) were rated as very good and diagnostic, while only 5 (10%) mSENSE data sets and only 1 (2%) GRAPPA data set yielded the best score.

Aliasing Artifacts

Unaccelerated VIBE images revealed no aliasing artifacts (mean score = 5.0 ± 0). Both PAT data sets were rated substantially worse. GRAPPA showed significantly more artifacts than mSENSE (3.68 ± 0.7 vs. 4.3 ± 0.6, $P < 0.001$ (Fig. 2). While 40 (82%) mSENSE image sets received the best rating, only 3 (6%) GRAPPA image sets were classified with a score of 5.

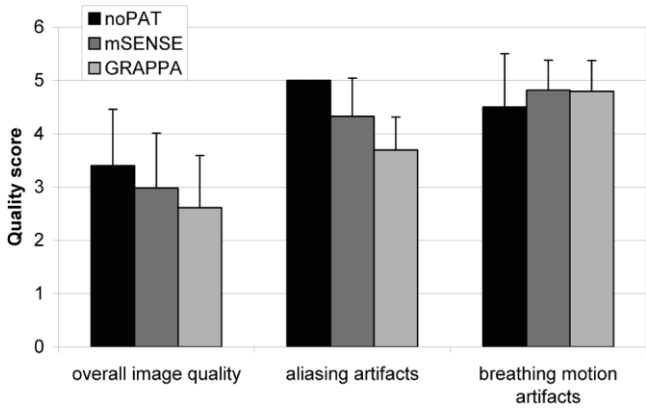

Figure 1. Quality scores of conventional VIBE sequence vs. mSENSE and GRAPPA reconstruction algorithms. Shown is mean ± SD. The accelerated images have a significantly ($P < 0.05$) lower mean score for overall image quality (GRAPPA, 2.60; mSENSE, 2.98) and aliasing artifacts (GRAPPA, 3.68; mSENSE, 4.3) than did the reference images (3.4 and 5.0, respectively). The scores for breathing motion artifacts showed a significant ($P < 0.05$) increase of mean score when the accelerated (GRAPPA, 4.82; mSENSE, 4.78) and reference images (4.52) were compared.

Respiratory Motion Artifacts

Both GRAPPA and mSENSE image sets were rated significantly better than the unaccelerated images (4.82 ± 0.56 ($P = 0.023$) and 4.78 ± 0.61 ($P = 0.046$), respectively, vs. 4.52 ± 1.0). There was no significant difference between the two PAT algorithms ($P = 1.0$). Ten (20%) mSENSE and 9 (18%) GRAPPA image sets were rated with a higher score than unaccelerated VIBE images. Indeed, 10 of 49 patients had difficulties holding their breath for the acquisition of the unaccelerated data sets. In these patients, PAT improved the breathing artifact severity score from 2.9 ± 1.0 to 4.1 ± 0.94 for GRAPPA and 4.2 ± 0.98 for mSENSE. Overall image quality was better for mSENSE (3.2 ± 0.91) than for unaccelerated images (2.9 ± 0.95) in these patients. GRAPPA images remained poorer in quality due to aliasing artifacts (2.7 ± 0.96). Figure 3 demonstrates conventional and accelerated images in a patient with reduced breath-holding capabilities.

Quantitative Evaluation of SNR and CNR

Conventional VIBE image data sets were characterized by significantly higher SNR values (mean = 50.8 ± 20.3) than GRAPPA (mean = 34.8 ± 14.0, $P < 0.001$) and mSENSE (mean = 33.0 ± 13.3, $P < 0.001$). Mean SNR decreased about 35% with both PAT techniques. However, the SNR of the accelerated images, compared with that of the unaccelerated images, may have been reduced somewhat owing to clearance of the contrast material during the interval between the two data acquisitions. Conversely, the difference between the two PAT reconstruction algorithms failed to prove statistical significance ($P = 0.173$).

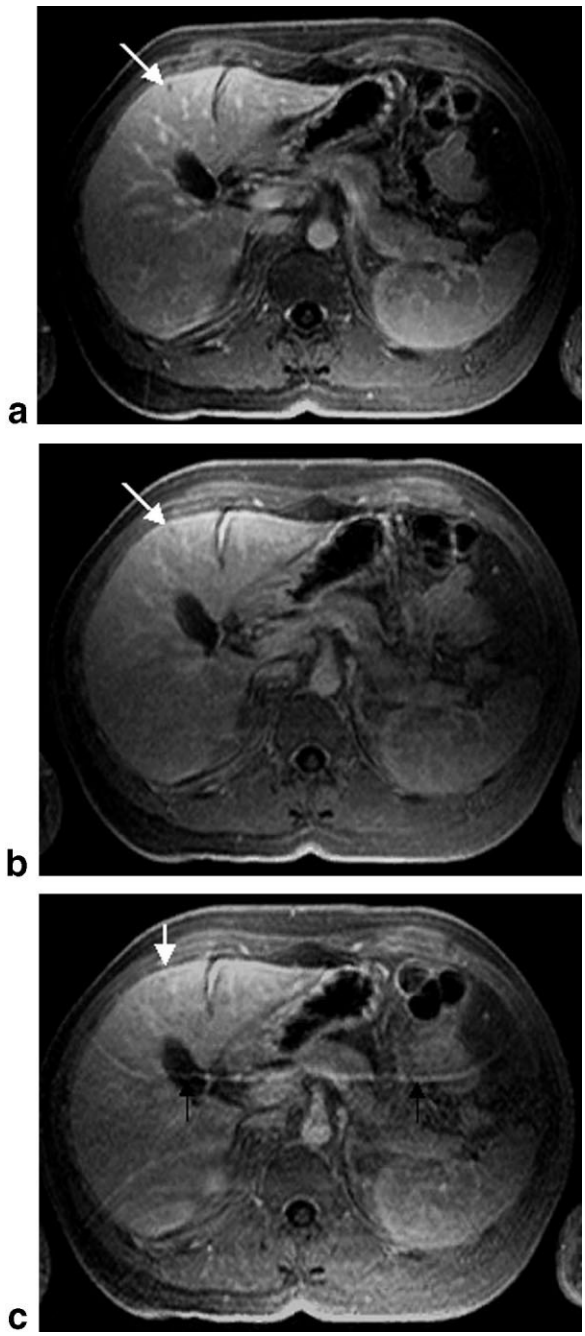

Figure 2. Images of a patient with a small liver lesion in the right liver lobe (white arrow): conventional (noPAT) VIBE sequence (**a**), mSENSE (**b**), and GRAPPA (**c**) reconstruction algorithms. Note the typical band-like fold-over artifacts in the GRAPPA image (c) (black arrows). Moreover, the increase in noise over the PAT images hinders detection of the small liver lesion (white arrow).

Quantitative CNR analysis revealed similar results: conventional VIBE images provided the highest CNR (mean = 32.6 ± 19.2), while both PAT reconstruction algorithms yielded significantly lower CNR values (GRAPPA, mean = 23.2 ± 15.0, $P < 0.001$; mSENSE, mean = 20.9 ± 12.7, $P = 0.04$). The differences between GRAPPA and mSENSE were not statistically significant ($P = 0.867$). Figure 4 compares the mean SNR and CNR values for the two different PAT reconstruction algorithms as well as conventional VIBE.

Lesion Detection

The reading based on all MRI data revealed 156 focal hepatic lesions in 32 of 49 patients. The unaccelerated late venous phase VIBE sequence revealed 146 lesions in the same patients. Retrospective analysis established all missed lesions to represent homogeneously enhancing metastases or focal nodular hyperplasia

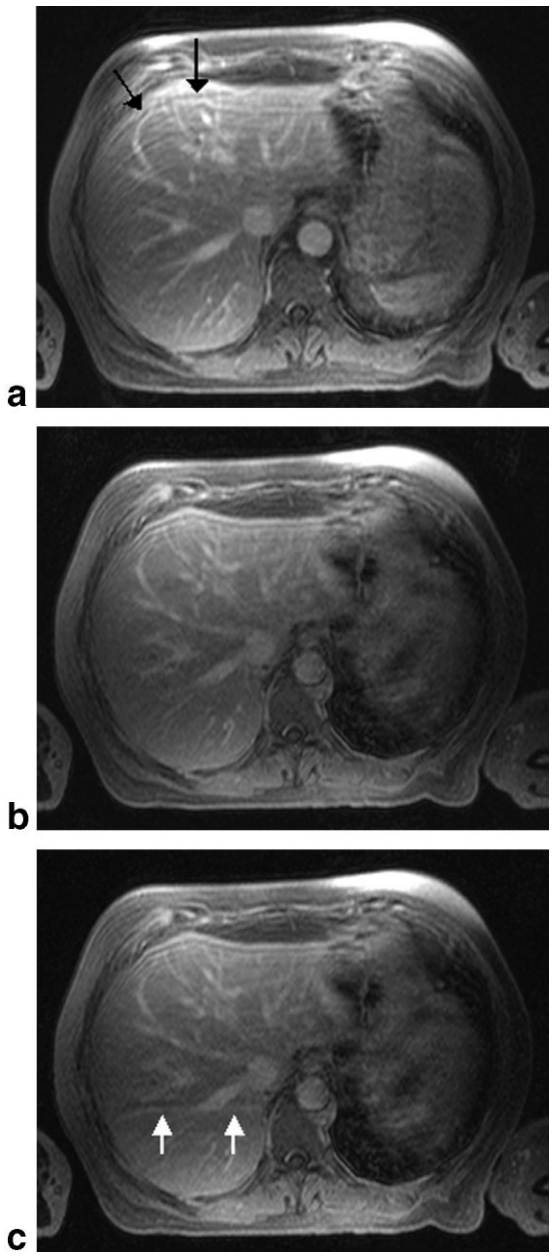

Figure 3. Images of the axial VIBE sequences: conventional (noPAT) (**a**), mSENSE (**b**), and GRAPPA (**c**) reconstruction algorithms. Note the reduced motion breathing artifacts (black arrows) in accelerated images in a patient who was unable to hold his breath during the conventional acquisition time. A typical band-like aliasing artifact is seen in the GRAPPA image crossing the dorsal parts of the liver (white arrows).

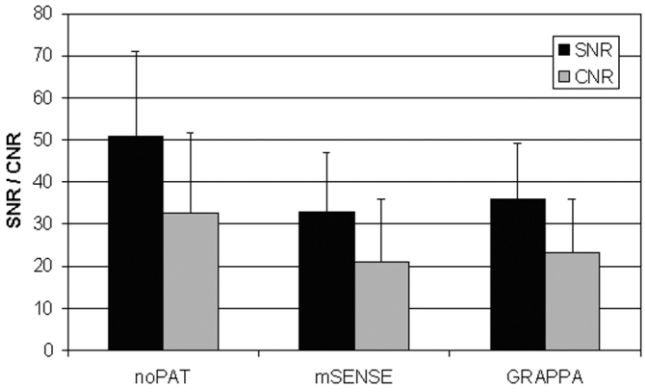

Figure 4. Comparison of overall SNR and CNR between the conventional VIBE sequence and the two different PAT reconstruction algorithms (mSENSE, GRAPPA). Shown is mean ± SD.

that could not be differentiated from surrounding normal liver in the late venous phase, but could be detected in earlier phases of the dynamic scan. Accelerated images with mSENSE reconstruction detected 138 lesions. GRAPPA revealed 127 lesions, and thus performed inferior to mSENSE. All lesions missed in the accelerated images but identified in the unaccelerated venous phase images were smaller than 4 mm in diameter. Only two of the overseen lesions in mSENSE and GRAPPA were retrospectively identified by a third reader. All others were not detectable due to poor image quality.

Compared to the unaccelerated late venous phase, mSENSE missed six of the eight lesions due to reduced SNR and two lesions due to artifacts. Using the GRAPPA algorithm, 5 of 19 missed lesions were not detectable due to reduced SNR and 14 due to fold-over artifacts. There were no false positive readings.

DISCUSSION

The present study evaluating the effect of twofold PAT acceleration on VIBE image quality and the ability to delineate hepatic lesions carries four messages we believe to be important:

1. Both PAT algorithms reduce image quality by introducing aliasing artifacts and decreasing SNR and CNR up to 35%.
2. Poorer image quality associated with PAT directly translates into poorer diagnostic performance regarding the detection of small (<4 mm diameter) focal hepatic lesions.
3. The mSENSE PAT algorithm generates fewer artifacts in abdominal imaging than GRAPPA.
4. Twofold PAT acceleration reduced the data acquisition time for a single three-dimensional image set covering the entire liver by 44% from 23 to 13 seconds. This reduction ensures dynamic three-dimensional VIBE image quality without respiratory motion artifacts even in patients with compromised respiratory function.

Not long after the introduction of multicoil arrays for MRI (10), various parallel acquisition strategies were proposed (11–13). Sodickson and Manning (7) first employed parallel imaging successfully for the purpose of reducing acquisition times in vivo. Depending on scanner performance, the PAT-induced shortening of data acquisition times can mean the difference between imaging in apnea and during free breathing. The avoidance of respiratory artifacts has a dramatically positive effect on image quality in the upper abdomen. Even in the presence of high-performance scanners like the one used in this study, PAT-induced reduction of imaging times can be very helpful. Thus, respiratory motion artifacts were reduced up to 30% using PAT in patients unable to hold their breath for the full 23 seconds required for conventional data collection. These results suggest that PAT will find its way into routine clinical protocols for patients with compromised respiratory function.

Earlier PAT studies in the abdomen were based on the PARS method (parallel imaging with augmented radius in k-space), using all acquired SI data within a specified radius from the k-space coordinate of an omitted SI datum to reconstruct missing data. Evaluations of PARS imaging in the liver revealed aliasing artifacts emanating from the abdominal wall, leading to a reduction of image quality (14,15). The technique employed in the PARS study shared one of the potential limitations of all externally calibrated imaging techniques—namely, that patient motion occurring between the time of the sensitivity reference scan and the accelerated scan could result in miscalibrations and resultant aliasing artifacts. New self-calibrating reconstruction algorithms like GRAPPA and mSENSE promise to overcome this limitation: additional k-lines in the center of k-space for self-calibration of coil sensitivities in each image are acquired during the data acquisition of the accelerated scan itself. Hence, the need for an a priori reference is eliminated, thereby avoiding the problems associated with mismatches.

Nevertheless, aliasing artifacts were still found in this study, especially when using the GRAPPA algorithm. To our knowledge, these artifacts are related to the use of standard array coils with limited numbers of array elements, which have not been optimized for parallel imaging. The algorithms are expected to benefit from increasing numbers of array elements, with the additional capability to more optimally image in a variety of imaging planes. With only four elements, the range of possible slice orientations and phase encoding directions is rather limited.

Dobritz et al (16) reported encouraging early clinical results when applying mSENSE to exams of the upper abdomen in a small study population. While the autocalibrating algorithms can reduce PAT-induced aliasing, they are far from eliminating it. Furthermore, PAT is known to reduce SNR and CNR in direct relationship to the reduction factor. Thus, the advantages of PAT related to the considerable reduction in data acquisition time, and hence the ability to vastly shorten the breath-holding requirements for dynamic imaging of the upper abdomen, must be weighed against potential costs related to poorer image quality. With this study,

we present a systematic investigation of two self-calibrating PAT algorithms on the diagnostic performance regarding the detection of focal hepatic lesions.

This study confirms that self-calibrating PAT reconstruction algorithms can be associated with substantial artifacts. Significantly more aliasing was seen in GRAPPA, whereas mSENSE provided diagnostic image quality in most cases. Reflecting the reduced SNR and CNR inherent to PAT, the accelerated images yielded a poorer mean score for overall image quality. Ignoring the autocalibration lines for SNR evaluation (which reflects the mSENSE case; for GRAPPA, see below), the SNR of the PAT acquisitions should theoretically = $SNR_{noPAT}/g\sqrt{R}$, where SNR_{noPAT} is the SNR without parallel acquisition, R is the acceleration factor (in this work R = 2), and g is a spatially dependent factor, dependent on the exact coil element geometry (8). The factor $\sqrt{R}$ results from the reduced number of excitations of the imaging plane. For GRAPPA, the SNR of the autocalibration lines can be incorporated into the final images. Therefore, the effective R with GRAPPA is less than 2, providing a slight theoretical SNR advantage over mSENSE. In practice, the measured difference between mean SNRs of GRAPPA (36 ± 14.0) and mSENSE (33 ± 13.3) was not statistically significant. Although the difference between mSENSE and GRAPPA failed to be statistically significant, these numbers confirm a trend toward 8% less SNR with mSENSE. With phased array coils specifically designed for parallel imaging, the g factor should more closely approach its ideal value of 1.

Since the g factor is spatially dependent, the noise background of parallel images varies with spatial position. Furthermore, recent studies have shown that the use of coil-by-coil magnitude images in techniques such as GRAPPA alters noise statistics such that traditional SNR estimation approaches and direct comparisons with other techniques can be unreliable (17). For both of these reasons, the SNR measurement method of separated ROIs used in the current study will not reflect the true SNR. One alternative method to minimize the influence of the nonuniformity on SNR is to collect two sequential acquisitions with identical imaging parameters, obtain the mean signal from an ROI on one of the images, and obtain a value for noise by the subtraction of one acquisition from the other (18). The application of this technique for calculation of SNR profiles in conjunction with PAT algorithms has shown a reduction in SNR by a factor of 25% to 40% compared to unaccelerated images, using an acceleration factor of 2 (19). Although it was not feasible to acquire two identical data sets for both algorithms in patients, we believe that our SNR results nevertheless give the clinicians an approximate overview of possible image quality reduction using the PAT algorithms.

Despite the slight theoretical SNR advantage of GRAPPA, the mSENSE reconstruction algorithm resulted in significantly higher mean scores for overall image quality, reflecting the increased frequency of fold-over artifacts associated with GRAPPA.

Poorer image quality due to less SNR/CNR and more artifacts directly translated into fewer detected lesions in the accelerated images. In particular, small lesions with a diameter of less than 4 mm were frequently missed. Again, the performance of GRAPPA was inferior to that of mSENSE. Based on these data, the use of PAT reconstruction algorithms with coil arrays, like the one used in this study, cannot be recommended for patients capable of holding their breath for the time required to collect an unaccelerated three-dimensional data set of the liver. Although the presented data do not provide definitive proof, it seems that PAT acceleration should nevertheless be considered in patients unable to hold their breath.

This study has several limitations. First and foremost, spatial resolution was kept constant to facilitate a comparative analysis. If the acquisition time were kept constant, pixel size could have been decreased from 2.1×1.6 mm^2 to 1.05×1.3 mm^2. The impact of improved spatial resolution on image quality was not explored. Furthermore, standard torso phased array coils were used. Since SNR and image quality for parallel MR images are closely tied to the geometry and sensitivity patterns of the coil arrays used for spatial encoding (20,21), all PAT strategies are expected to benefit from dedicated PAT coils with an increased number of array elements (22). Different parallel imaging array designs have been introduced by our scanner manufacturer and are currently being explored. With these coils, the rather disappointing results presented in this study are likely to improve. For those who do not have access to the newer coils, this study helps set the boundary conditions for the use of PAT for the detection of liver lesions.

In summary, we conclude that the achieved time savings due to PAT are associated with considerable compromises in image quality, including SNR and CNR reductions, as well as substantial aliasing artifacts, despite the use of self-calibrating reconstruction algorithms. Poorer image quality directly translates into poorer diagnostic performance regarding the detection of small hepatic metastases. Thus, the use of PAT in the abdomen should be limited to patients unable to hold their breaths for regular dynamically collected three-dimensional VIBE data sets. Newly developed coils dedicated for PAT imaging will probably overcome the exposed limitations.

REFERENCES

1. Whitney WS, Herfkens RJ, Jeffrey RB, et al. Dynamic breath-hold multiplanar spoiled gradient-recalled MR imaging with gadolinium enhancement for differentiating hepatic hemangiomas from malignancies at 1.5 T. Radiology 1993;189:863–870.
2. Hamm B, Thoeni RF, Gould RG, et al. Focal liver lesions: characterization with nonenhanced and dynamic contrast material-enhanced MR imaging. Radiology 1994;190:417–423.
3. Soyer P, de Givry SC, Gueye C, Lenormand S, Somveille E, Scherrer A. Detection of focal hepatic lesions with MR imaging: prospective comparison of T2-weighted fast spin-echo with and without fat suppression, T2-weighted breath-hold fast spin-echo, and gadolinium chelate-enhanced 3D gradient-recalled imaging. AJR Am J Roentgenol 1996;166:1115–1121.
4. Peterson MS, Baron RL, Murakami T. Hepatic malignancies: usefulness of acquisition of multiple arterial and portal venous phase images at dynamic gadolinium-enhanced MR imaging. Radiology 1996;201:337–345.
5. Carlson J, Crooks L, Ortendahl D, Kramer DM, Kaufman L. Signal-to-noise ratio and section thickness in two-dimensional versus three-dimensional Fourier transform MR imaging. Radiology 1988; 166:266–270.

6. Rofsky NM, Lee VS, Laub G, et al. Abdominal MR imaging with a volumetric interpolated breath-hold examination. Radiology 1999; 212:876–884.
7. Sodickson DK, Manning WJ. Simultaneous acquisition of spatial harmonics (SMASH): fast imaging with radiofrequency coil arrays. Magn Reson Med 1997;38:591–603.
8. Pruessmann KP, Weiger M, Scheidegger MB, Boesiger P. SENSE: sensitivity encoding for fast MRI. Magn Reson Med 1999;42:952–962.
9. Griswold MA, Jakob PM, Heidemann RM, et al. Generalized autocalibrating partially parallel acquisitions (GRAPPA). Magn Reson Med 2002;47:1202–1210.
10. Roemer PB, Edelstein WA, Hayes CE, Souza SP, Mueller OM. The NMR phased array. Magn Reson Med 1990;16:192–225.
11. Hutchinson M, Raff U. Fast MRI data acquisition using multiple detectors. Magn Reson Med 1988;6:87–91.
12. Kwiat D, Einav S, Navon G. A decoupled coil detector array for fast image acquisition in magnetic resonance imaging. Med Phys 1991; 18:251–265.
13. Ra JB, Rim CY. Fast imaging method using multiple receiver coils with subencoding data set. In: Procceedings of the SMRM, 10th Annual Meeting, San Francisco, 1991. p 1240.
14. McKenzie CA, Lim D, Morrin M, et al. Clinical evaluation of parallel imaging for accelerated VIBE MRI of the liver. In: Proceedings of the 10th Annual Meeting of ISMRM, Honululu, 2002.
15. McKenzie CA, Lim D, Ransil BJ, et al. Shortening MR image acquisition time for volumetric interpolated breath-hold examination with a recently developed parallel imaging reconstruction technique: clinical feasibility. Radiology 2004;230:589–594.
16. Dobritz M, Radkow T, Nittka M, Bautz W, Fellner FA. VIBE with parallel acquisition technique—a novel approach to dynamic contrast-enhanced MR imaging of the liver [in German]. Rofo Fortschr Geb Rontgenstr Neuen Bildgeb Verfahr 2002;174:738–741.
17. Yeh EN, McKenzie CA, Grant AK, Ohliger MA, Willig-Onwuachi JD, Sodickson DK. Generalized noise analysis for magnitude image combinations in parallel MRI. In: Proceedings of the 11th Annual Meeting of ISMRM, Toronto, Canada, 2003. p 6.
18. Firbank MJ, Coulthard A, Harrison RM, Williams ED. A comparison of two methods for measuring the signal to noise ratio on MR images. Phys Med Biol 1999;44:N261–N264.
19. Maderwald S, Barkhausen J, Quick HH, et al. SNR Comparison between parallel acquisition techniques GRAPPA and mSENSE. In: Proceedings of the 10th Annual Meeting of ISMRM, Honululu, 2002. p 358.
20. Sodickson DK, McKenzie CA, Ohliger MA, Yeh EN, Price MD. Recent advances in image reconstruction, coil sensitivity calibration, and coil array design for SMASH and generalized parallel MRI. Magma 2002;13:158–163.
21. Pruessmann KP, Weiger M, Boesiger P. Sensitivity encoded cardiac MRI. J Cardiovasc Magn Reson 2001;3:1–9.
22. Weiger M, Pruessmann KP, Leussler C, Roschmann P, Boesiger P. Specific coil design for SENSE: a six-element cardiac array. Magn Reson Med 2001;45:495–504.